

Article

Discovery of Disulfane (H₂S₂) in Fluid Inclusions in Rubies from Yuanjiang, China, and Its Implications

Wenqing Huang^{1,2}, Pei Ni^{2,*} , Jungui Zhou¹, Ting Shui³, Junying Ding², Renzhi Zhu⁴, Yitao Cai³ and Mingsen Fan²

¹ National Center of Inspection and Testing on Quality of Gold and Silver Products, Nanjing Institute of Product Quality Inspection, Nanjing 210019, China; huangwq@smail.nju.edu.cn (W.H.); zhou_jungui@163.com (J.Z.)

² State Key Laboratory for Mineral Deposits Research, Institute of Geo-Fluids, School of Earth Sciences and Engineering, Nanjing University, Nanjing 210093, China; jyding@nju.edu.cn (J.D.); dg1629010@smail.nju.edu.cn (M.F.)

³ Nanjing Center, China Geological Survey, Nanjing 210016, China; vansting@vip.sina.com (T.S.); cyitao@cgs.cn (Y.C.)

⁴ CAS Key Laboratory of Crust-Mantle Materials and Environments, School of Earth and Space Sciences, University of Science and Technology of China, Hefei 230026, China; renzhizhu@ustc.edu.cn

* Correspondence: peini@nju.edu.cn

Abstract: Raman spectra of fluid inclusions in gem rubies from Yuanjiang deposit (China) within the Ailao Shan-Red River (ASRR) metamorphic belt showed the presence of compounds such as CO₂, COS, CH₄, H₂S, and elemental sulfur (S₈), accompanied by two bands at approximately 2499 and 2570 cm⁻¹. These two frequencies could be assigned to the vibrations of disulfane (H₂S₂). This is the second case of the sulfane-bearing fluid inclusions in geological samples reported, followed by the first in quartzite from Bastar Craton of India. The H₂S₂ was likely in situ enclosed by the host rubies rather than a reaction product that formed during the cooling of H₂S and S₈, suggesting sulfanes are stable at elevated temperatures (e.g., >600 °C). By comparing the lithologies and metamorphic conditions of these two sulfane-bearing cases (Bastar and Yuanjiang), it is suggested that amphibolite facies metamorphism of sedimentary sequence that deposited in a continental platform setting might favor the generation of sulfanes. Sulfanes may play an important role in the mobilization of Cr that is essential for ruby crystallization.

Keywords: rubies; fluid inclusion; Ailao Shan-Red River metamorphic belt



Citation: Huang, W.; Ni, P.; Zhou, J.; Shui, T.; Ding, J.; Zhu, R.; Cai, Y.; Fan, M. Discovery of Disulfane (H₂S₂) in Fluid Inclusions in Rubies from Yuanjiang, China, and Its Implications. *Crystals* **2021**, *11*, 1305. <https://doi.org/10.3390/cryst11111305>

Academic Editor: Francesco Capitelli

Received: 28 September 2021

Accepted: 25 October 2021

Published: 27 October 2021

Publisher's Note: MDPI stays neutral with regard to jurisdictional claims in published maps and institutional affiliations.



Copyright: © 2021 by the authors. Licensee MDPI, Basel, Switzerland. This article is an open access article distributed under the terms and conditions of the Creative Commons Attribution (CC BY) license (<https://creativecommons.org/licenses/by/4.0/>).

1. Introduction

Numerous volatile species (e.g., CO₂, CO, O₂, C₃H₈, and N₂) in fluid inclusions are well documented in the literature [1]. Sulfur, an element with redox states ranging from −2 to +6, can be found in fluid inclusions as sulfur compounds of different valence, e.g., S₈, COS, SO₂, and H₂S in gaseous, and SO₄^{2−}, HSO₄[−], and HS[−] solutes in aqueous fluids [1,2]. Polysulfanes (H₂S_n with n > 1; or hydrogen polysulfides) are generally found in natural gas and crude sulfane oils [3], but their presence in natural fluid inclusions is rare. Recently, disulfane (H₂S₂) was described for the first time in natural CH₄–H₂S inclusions in Archaean quartzite from Bastar Craton of India [4]; recognition and assignment of the H₂S₂-related Raman bands was accomplished according to quantum chemical calculations based on the density functional theory. Given that sulfanes have been observed in both sulfur-bearing fluid inclusions and sulfur-free types, the possibility that disulfane formed by the post-entrapment reaction between molten sulfur and H₂S was ruled out by Hurai et al. [4]. They accordingly inferred that the disulfane or any other unknown S–H-bearing species that could dissociate into disulfane along the cooling path should be present before the fluid was trapped by quartz. This is critical to understanding the fluid process and is thus of significance to investigate. On the other hand, many aspects regarding H₂S₂, e.g.,

the favorable formation condition, thermochemical stability, and its potential roles in the mobilization of specific elements, remain largely unclear and require further investigation.

For marble-hosted ruby deposits from Central and Southeast Asia, studies on fluid inclusions show that sulfur-bearing fluids with the composition of $\text{CO}_2\text{-H}_2\text{S}$ ($\pm\text{COS} \pm \text{S}_8$) occurred during corundum growth [2,5]. These complex fluids are metamorphic in origin and can be explained by decarbonation of limestone (CO_2) and reduction in sulfate (elemental sulfur, hydrogen sulfide, and COS) [2].

Here, we report the second occurrence of H_2S_2 composition in ruby-hosted fluid inclusions from the Ailao Shan-Red River (ASRR) metamorphic belt. It corroborates the presence of sulfanes in high-grade metamorphic fluids. We further discussed its origin, thermochemical stability, and geochemical implications.

2. Geological Setting

The geology of the ASRR metamorphic belt has been documented in some detail by Tapponnier et al. [6] and Leloup et al. [7]. The ASRR metamorphic belt, a Tertiary left-lateral strike-slip fault zone, is traditionally interpreted to play an important role in the accommodation of the extrusion of the Indochina block during the India–Eurasia collision (Figure 1) [6,7]. The elongate Ailao Shan metamorphic massif is composed of mylonitic gneisses, migmatites, granitic pods, amphibole-bearing alkaline intrusions, and marble boudins [8,9]. U–Pb ages of zircon, xenotime, titanite from syntectonic leucogranites combined with Ar–Ar radiometric dating of biotite, muscovite, and K-feldspar within the Ailao Shan set the timing of left-lateral shearing activity from 35 Ma to 17 Ma [7–9]. In addition, 23.4 ± 0.3 Ma U–Pb ages of titanite syngenetic with rubies in marbles from Yuanjiang, which recorded the age of ruby mineralization, are also within this range [10]. Peak metamorphism occurred at 4.5 ± 1.5 kbar and 710 ± 70 °C, as revealed by a petrographic investigation on Ailao Shan massif [11]. Greenschist facies retrograde metamorphism occurred at pressures (P) of <3.8 kbar and temperatures (T) around 500 °C [11].

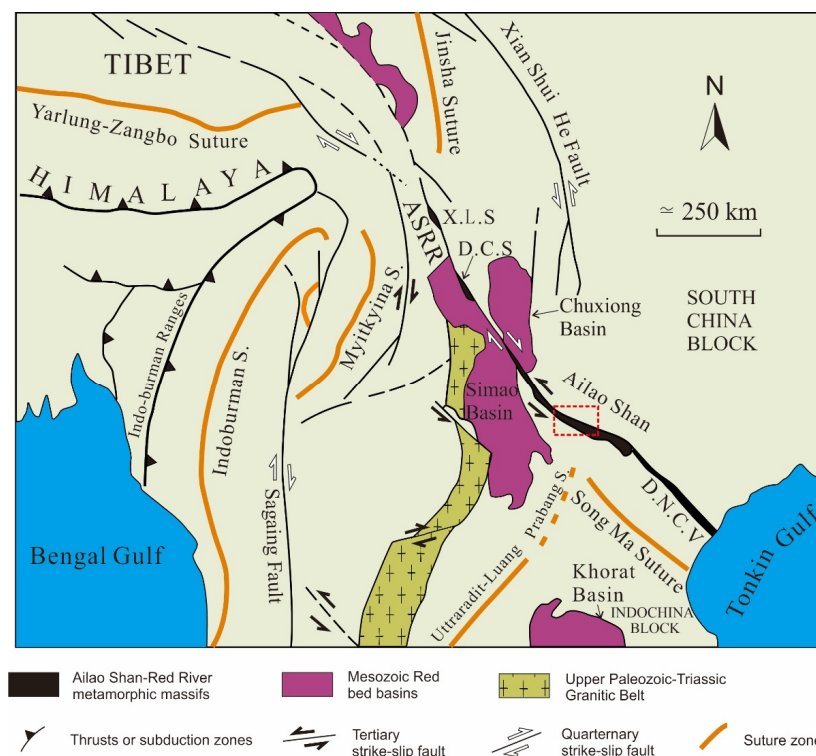


Figure 1. Simplified tectonic sketch of SE Asia showing the ASRR metamorphic terranes (modified after Leloup et al. [7]) with marked study area. The ASRR strike-slip metamorphic zone is comprised of four metamorphic terranes: Ailao Shan, Xuelong Shan (XLS), Diancang Shan (DCS), and Day Nui Con Voi (DNCV).

3. Materials and Methods

Corundum-bearing marbles in this investigation are from the Yuanjiang region in the central segment of the Ailao Shan mountain (Figure 2). They are exposed as boudins within meta-sedimentary hosts including gneiss, amphibolite, and leptynite. The marbles are medium- to coarse-grained in size and white and light gray in color. Most marble mainly comprises calcite with small amounts of micas, feldspars. Other minerals identified in marbles include ruby, rutile, spinel, sphene, graphite, pyrrhotite, and pyrite.

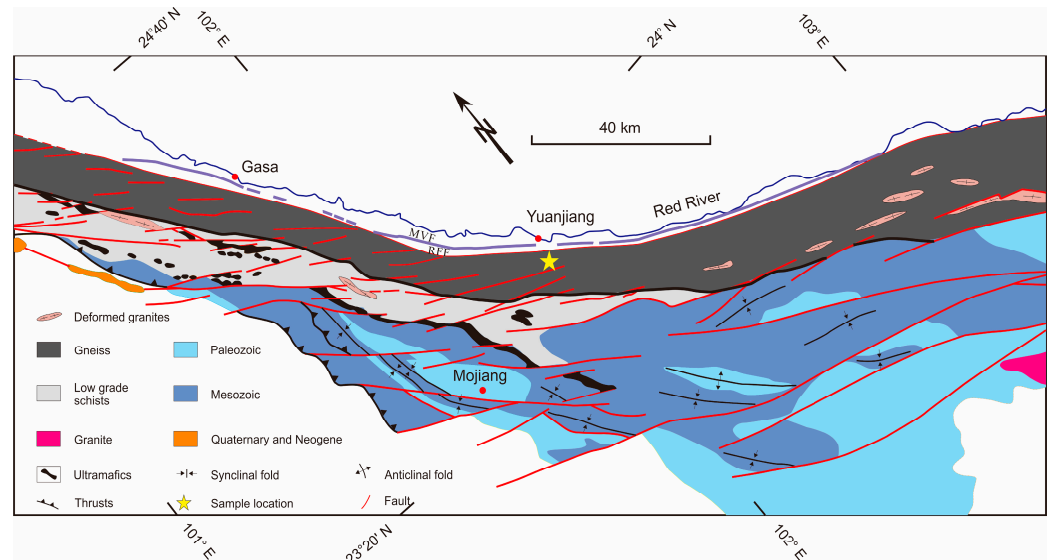


Figure 2. Structural map of Ailao Shan metamorphic range (modified after Leloup et al. [7]); MVF—mid-valley fault; RFF—range front fault.

We conducted fluid inclusion studies on both primary rubies in the marble matrix and secondary rubies (Figure 3) recovered from the sediments around the village of Shaku in Yuanjiang County. These ruby fragments were cut and doubly polished to a thickness of 150–200 μm . An optical microscope was used for petrographic observation of fluid inclusions. In addition, four pieces of ruby-bearing marbles were doubly polished for fluid inclusions investigations.

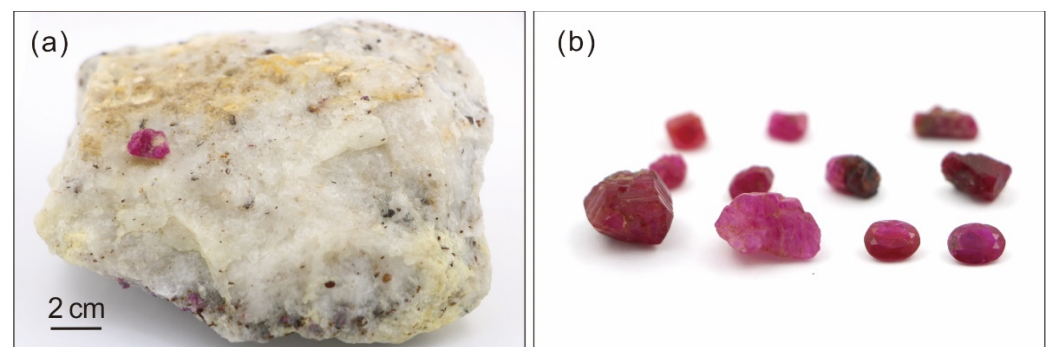


Figure 3. (a) Ruby-bearing marble and (b) secondary rubies (0.50–5 ct) from Yuanjiang, China.

Raman analyses on fluid inclusions were completed at HORIBA Instrument (Shanghai) Co., Ltd., employing a confocal LabRAM HR Evolution Raman microspectrometer (Horiba, Ltd., Kyoto, Japan) coupled to an Olympus BX-51 microscope. Raman spectra were collected with a 100 \times objective lens. To suppress fluorescence from the host ruby, a 473 nm excitation wavelength of 25 mW, air-cooled solid-state Nd-YAG laser was selected, allowing detection of bands above 1500 cm^{-1} . The analytical settings included 600 grooves/mm

gratings, 10–20 s acquisition time, and 2–3 times accumulations. Spectra processing was performed with baseline correction unless otherwise specified. Daily calibration of the spectrometer was completed with a monocrystalline silicon wafer (520.7 cm^{-1}).

4. Results

The fluid inclusions can be subdivided into three types according to their entrapment sequence relative to ruby growth, i.e., primary, pseudo-secondary, and secondary. A detailed description of fluid inclusion classification was given in Huang et al. [10] and is briefly outlined in Table 1. Mostly, these fluid inclusions are approximately 20–60 μm in diameter (Figure 4). Raman analyses showed complex fluid composition in the primary and pseudo-secondary fluid inclusions (Figures 4 and 5); they comprise CO_2 , H_2S , COS , S_8 , and CH_4 (Figure 5). Components such as CO_2 , H_2S , COS , S_8 , and CH_4 were also observed in the fluid inclusions of secondary origin. Moreover, solids in the fluid inclusions cavities, identified by Raman spectroscopy, include diaspore, arsenopyrite, dawsonite, gibbsite, pyrite, and rutile (Figures 4 and 5 and Table 1).

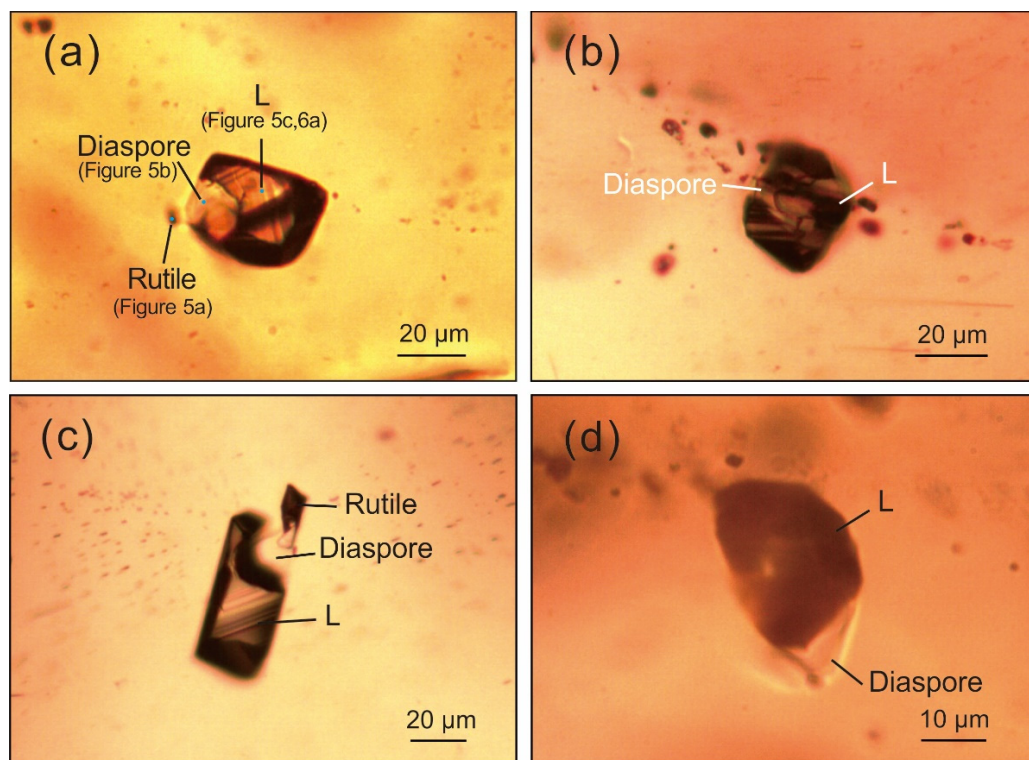


Figure 4. Photomicrographs of H_2S_2 -bearing fluid inclusions. These fluid inclusions sometimes contain rutile crystals (a,c) and diaspore crystals (a–d): L—liquid carbonic phase.

Table 1. Summary of occurrences and components of various types of fluid inclusion in Yuanjiang rubies.

Inclusion Types	Occurrence Description	Fluid Components	Solids
Primary	Oriented clusters throughout the host or small clusters in the core of the host, sometimes occurred as isolated or clusters within colored growth zonation	CO_2 – H_2S – COS – S_8 – H_2S_2 – CH_4	Diaspore, gibbsite, dawsonite, rutile, and arsenopyrite
Pseudo-secondary	In intragranular fractures that do not traverse into the rim of the host	CO_2 – H_2S – COS – S_8 – H_2S_2 – CH_4	Diaspore, arsenopyrite, and pyrite
Secondary	In sealed fractures present in planar arrays that traversed The growth zone of crystals	CO_2 – H_2S – COS – S_8 – CH_4	Diaspore

Moreover, two Raman bands at 2499 and 2570 cm^{-1} were observed in fluid inclusions of both primary and pseudo-secondary origins (Figure 5).

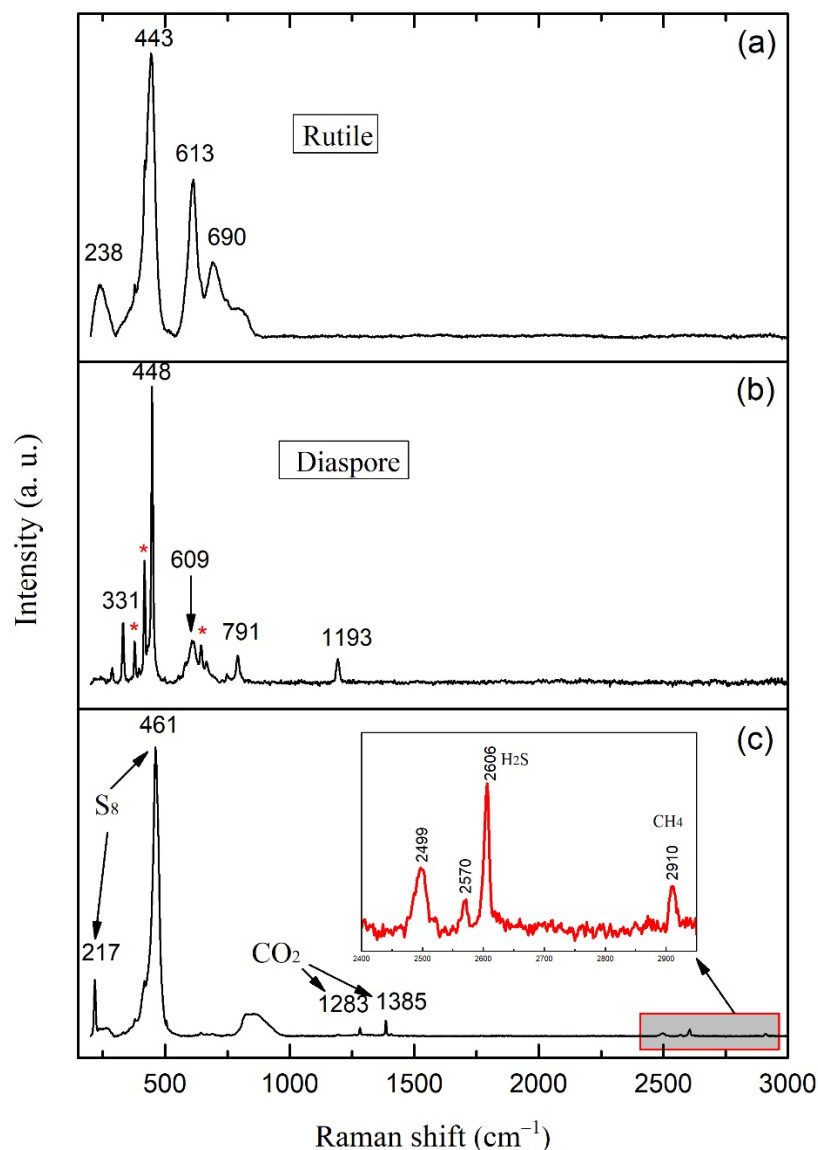


Figure 5. Raman spectra of the fluid inclusion as shown in Figure 4a: (a) the Raman spectrum corresponds to rutile; (b) Raman spectra showed that the transparent crystal was diaspore. Asterisk denoted the Raman signals from the hosting corundum; (c) the components of the included fluid included native sulfur (S_8), CO_2 , H_2S , and CH_4 . Two bands centered at 2499 and 2570 cm^{-1} can be clearly seen.

5. Discussion

5.1. Identification of Disulfane

The density functional theory method is a useful method for molecular structure prediction [3]. It is especially suitable for unstable reactive species (e.g., sulfur-rich compounds) whose structures and spectroscopic properties can hardly be obtained experimentally. Hurai et al. [4] employed the B3LYP hybrid functional and the basis set correlation-consistent polarized valence triple-zeta (cc-pVTZ) for the Raman frequency calculations of the polysulfanes. Quantum chemical calculations of both pure H_2S_n ($n = 2-6$) compounds and S_8 -sulfane interactions had been conducted by these authors. They observed a similar pattern between the theoretical Raman bands of various systems comprising S_8 -polysulfane and the examined sulfur-bearing fluid inclusions. Accordingly, they indicated that the

2488 cm^{-1} Raman band corresponds to H-bonded S-H stretch vibrations of the $\text{H}_2\text{S}_2 \cdots \text{S}_8 \cdots \text{H}_2\text{S}_2$ complex, whereas the 2503 cm^{-1} band corresponds to non-H-bonded S-H stretching vibration of the $\text{H}_2\text{S}_2 \cdots \text{S}_8$ complex. Another band at 2574 cm^{-1} was interpreted to reflect S-H stretch vibration in $\text{H}_2\text{S} + \text{H}_2\text{S}_2 \cdots \text{S}_8$ [4].

Fluid inclusion in marble-hosted rubies from Central and Southeast Asia have been extensively studied [2,5]. However, the 2499 and 2570 cm^{-1} Raman bands, which have not been detected in rubies from other deposits, are the most notable features of Raman bands of the investigated fluid inclusions within Yuanjiang rubies. The pioneering work of sulfane-bearing fluid inclusions carried out by Hurai et al. [4] enables us to interpret these two Raman bands. Deconvolution of the broad peak at 2499 cm^{-1} using PeakFit software (version 4.12) revealed two bands centered at 2484 and 2499 cm^{-1} (Figure 6c). Hurai et al. [4] have shown the broadband around 2497 cm^{-1} actually comprised two peaks centered at 2482–2488 cm^{-1} and 2497–2499 cm^{-1} . Therefore, the two bands of 2484 and 2499 cm^{-1} observed in Yuanjiang rubies could be ascribed to H_2S_2 -related vibrations and positively identified the presence of sulfanes.

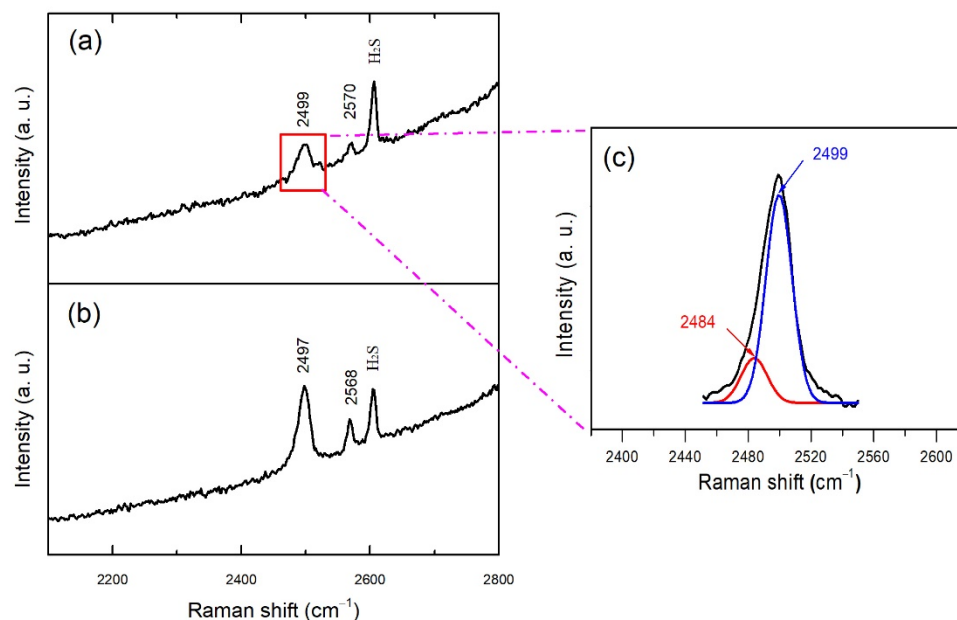


Figure 6. Raman spectra of fluid inclusions showing the H_2S_2 -related bands at approximately 2499 and 2570 cm^{-1} : (a) Raman spectrum without baseline correction of the inclusion as shown in Figure 4a; (b) Raman spectrum without baseline correction of the inclusion as shown in Figure 4b; (c) deconvolution of the 2499 cm^{-1} band reveals a hidden band centered at 2484 cm^{-1} . The bands at 2484 and 2499 cm^{-1} reflect the respective H-bonded and non-H-bonded SH-stretching vibrations of the $\text{H}_2\text{S}_2 \cdots \text{S}_8 \cdots \text{H}_2\text{S}_2$ complex.

5.2. Origin of Sulfane in Yuanjiang Rubies

The sulfur–sulfur bonds in S_8 have rather a high bond enthalpy (264 kJ mol^{-1}), which results in sulfur atoms forming as chains, rings, or clusters in numerous compounds [3]. Sulfanes, H_2S_n , are among the most basic of such species. However, reports regarding the natural occurrences of sulfanes are still limited; they typically occur in crude sulfane oils [3]. Moreover, they could be found in hot underground deposits of natural gas where H_2S and elemental sulfur coexist [3] and sulfur-containing hydrothermal environments [12–14]. Both elemental sulfur and H_2S are common species coexisting in fluid inclusions [2,5], and sulfanes can be produced by the interaction of S_8 with H_2S via the reaction $\text{H}_2\text{S}_n + n\text{S}_{\text{liq}} \rightarrow \text{H}_2\text{S}_{n+1}$ [3]; however, their presence in fluid inclusions is still very rare. Thus far, the sulfane in fluid inclusions has been only reported in Archaean mica-rich quartzite from near the Saigon village within the Bastar Craton, India [4], to the best of our knowledge. These authors inferred that the H_2S_2 (or its precursor sulfur-bearing species) could have

been present during the quartz crystallization, as the H_2S_2 -related Raman bands could be detected in sulfur-free CH_4-H_2S inclusions [4].

The coexistence of hydrogen sulfide and elemental sulfur is also a common characteristic of marble-hosted rubies from Central and Southeast Asia [5]. However, in addition to the Yuanjiang rubies, H_2S_2 has not been identified in any other deposits [2,5]. The Asian marble-hosted rubies formed under similar geological processes during the Cenozoic Himalayan orogenesis. Garnier et al. [15] suggested that they formed under amphibolite facies conditions. Since H_2S_2 has not been detected in other Asian marble-hosted rubies, it seems reasonable to infer that H_2S_2 in sulfur-bearing inclusions within Yuanjiang rubies does not result from a post-entrapment reaction between the elemental sulfur and the coexisting H_2S -bearing fluid. On the contrary, a most plausible explanation for its occurrence could be that H_2S_2 or its precursor mixed-valence sulfur-bearing species should have been present during the crystallization of Yuanjiang rubies.

Though the ASRR shear belt probably activated as a lithosphere-scale ductile strike-slip shear zone in the Tertiary [16], mantle-derived rocks have not been found within the mylonitic gneisses shear belt thus far [11]. Available evidence obtained from biotite-garnet and plagioclase-garnet thermobarometers suggests that the exhumed terrane along this belt corresponds to a paleo-depth of about 18 km [11]. The protoliths of the Ailao Shan high-grade metamorphic massif are of sedimentary origin [17]. Assuming a crustal thickness of 35–40 km for the study area [11,18], these observations suggest that rubies have a mid-crustal origin. As the sulfane composition in fluid inclusions is speculated to be enclosed during ruby growth (sulfane-bearing fluid inclusions are primary and pseudo-secondary), it must also have a mid-crustal origin.

5.3. Favorable Geological Condition for the Generation of Sulfanes

At both localities where H_2S_2 was detected (Bastar Craton in India and Ailao Shan metamorphic massif in China), rock types and metamorphic grades are comparable. The first documented sulfane-bearing fluid inclusions from India were found in metasedimentary sequence, which predominates in gneisses and contains minor schists, quartzites, marbles, and metabasalts. Peak metamorphism in this region occurred at amphibolite facies [4]. As for the Yuanjiang area, peak P-T conditions also correspond to amphibolite facies [11] and the exposed rocks are mainly composed of gneisses accompanied with some migmatites and granitic pods, and interlayers of metapelites, amphibolite, and marble.

Comparison of the lithologies and P-T conditions between these two examples suggests amphibolite facies metamorphism of sedimentary sequence that deposited in a continental platform setting is favorable for the generation of H_2S_2 . Even in similar-facies metamorphic terranes, the conditions can be very different in terms of fluid compositions, retrograde paths, and timeframes, etc., which may explain the H_2S_2 deficiency in fluid inclusions from other rubies in metasedimentary sequences. This explains the singularity of the localities where sulfanes have been found. Unfortunately, the specific mechanism for the generation of sulfanes in the above two occurrences remains unclear.

5.4. Implication for Thermochemical Stability of Sulfanes

If the explanation about H_2S_2 (or its precursor S-H-bearing species) formation was plausible, this would imply that the sulfanes or its precursor mixed-valence sulfur-bearing species could remain stable in metamorphic conditions of Yuanjiang corundum formation. The P-T estimates for the Yuanjiang ruby crystallization remain unconstrained at present. At another marble-hosted ruby deposit in the ASRR metamorphic belt, located in the Day Nui Con Voi range in Vietnam, the ruby mineralization temperature is calculated in the range of 600 to 625 °C by calcite-graphite isotopic thermometry [19]. Here, we assumed that the Yuanjiang rubies formed at a similar temperature range. This high formation temperature of Yuanjiang ruby implies that the thermochemical stability of sulfanes or its precursor S-H-bearing species could be as high as 600 °C. Thus far, there are few experiments and thermodynamic calculations to establish the stability limits of sulfanes in

natural fluid systems. Migdisov et al. [14] have experimentally shown that sulfanes remain stable at temperatures of 200–290 °C. However, the wider-range P-T stability of sulfanes is still unavailable. Nevertheless, based on their inference that H₂S₂ or its precursor sulfur-bearing compounds could have been present during the quartz crystallization, Hurai et al. [4] suggested high-temperature stability for mixed-valence sulfur-bearing species (>400 °C as estimated by graphite thermometer using Raman spectrometric method). If our inference is correct, it considerably expands the temperature stability of H₂S₂ or its precursor species. The presence of even traces of water tend to contribute to the decomposition of H₂S₂ [3]; though sulfanes and water were simultaneously present during entrapment in Yuanjiang rubies, water had been exhausted completely by reactions with the host corundum to produce diaspore along the cooling P-T path [10], making the preservation of sulfanes possible.

5.5. Geochemical Implications

The geological features at Yuanjiang share some similarities with those observed at the Bastar Craton region of India, where the sulfane-bearing inclusions were first documented. For example, they both occur in the high-grade gneissic terrane. Moreover, Cr-rich minerals were found in both of these locations, as represented by Cr-rich mica (up to 1.8 wt.% Cr₂O₃) and Cr-chlorite in Bastar [4], and ruby in Yuanjiang (up to 1.1 wt.% Cr₂O₃) [20], respectively.

Chromium, a siderophile element essential for the formation of rubies, is commonly considered as immobile in most geological fluids [21]. Short-distance mobilization of Cr has been proposed by molten salts during the ruby formation [5]. In other cases, it has been demonstrated that the polysulfide complexation in hydrothermal fluids plays an important role in transporting siderophile elements [22]. If our inference that sulfanes or its precursor S-H-bearing species were present in the course of Yuanjiang ruby precipitation is valid, then the role of sulfanes (or its precursor) in Cr mobilization could be expected.

6. Conclusions

The identification of H₂S₂ fluid composition in rubies from Yuanjiang marbles is the second example of sulfane-bearing fluid inclusions after quartz hosted H₂S₂-bearing fluids, confirming the presence of sulfane in geological fluids at elevated P-T conditions. Our observations suggest that H₂S₂ or its precursor S-H-bearing species should have been present during the Yuanjiang ruby precipitation. This further implies that sulfanes can survive high P-T and probably result from the amphibolite facies metamorphism of the sedimentary sequence. The presence of reduced volatiles such as H₂S₂ also provides robust evidence for corundum crystallization in a reduced condition [13], aligning with the presence of H₂S and CH₄ in the fluid phase of Yuanjiang rubies.

Author Contributions: Conceptualization, W.H., P.N. and T.S.; methodology, W.H. and J.D.; validation, R.Z. and M.F.; formal analysis, W.H., R.Z., Y.C. and M.F.; investigation W.H., R.Z. and M.F.; writing—original draft preparation, W.H.; writing—review and editing, P.N., J.Z. and T.S.; supervision, P.N., T.S. and J.Z.; funding acquisition, P.N. and J.D. All authors have read and agreed to the published version of the manuscript.

Funding: This research was funded by the National Key R&D Programme of China (2018YFA0702704), Natural Science Foundation of Jiangsu Province (BK20201258), and Science and Technology Program of Nanjing Administration for Market Regulation (KJ2019005).

Data Availability Statement: Not applicable.

Acknowledgments: The authors want to thank Enping Hu and Peng Xu from HORIBA Instrument (Shanghai) Co., Ltd. for their help with Raman analysis. They are also thankful to Yulong Yang from College of Earth Science and Key Laboratory of Tectonic Controlled Mineralization and Oil Reservoir, Chengdu University of Technology, and Zhongping Yang for their assistant during the fieldwork.

Conflicts of Interest: The authors declare no conflict of interest.

References

1. Frezzotti, M.L.; Tecce, F.; Casagli, A. Raman spectroscopy for fluid inclusion analysis. *J. Geochem. Explor.* **2012**, *112*, 1–20. [[CrossRef](#)]
2. Giuliani, G.; Dubessy, J.; Banks, D.; Hoàng Quang, V.; Lhomme, T.; Pironon, J.; Garnier, V.; Phan Trong, T.; Pham Van, L.; Ohnenstetter, D.; et al. CO₂–H₂S–COS–S₈–AlO (OH)-bearing fluid inclusions in ruby from marble-hosted deposits in Luc Yen area, North Vietnam. *Chem. Geol.* **2003**, *194*, 167–185. [[CrossRef](#)]
3. Steudel, R. Inorganic Polysulfanes H₂S_n with n > 1. In *Elemental Sulfur und Sulfur–Rich Compounds II*; Steudel, R., Ed.; Springer: Berlin/Heidelberg, Germany, 2003; pp. 99–125.
4. Hurai, V.; Černušák, I.; Randive, K. Raman spectroscopic study of polysulfanes (H₂S_n) in natural fluid inclusions. *Chem. Geol.* **2019**, *508*, 15–29. [[CrossRef](#)]
5. Giuliani, G.; Dubessy, J.; Banks, D.A.; Lhomme, T.; Ohnenstetter, D. Fluid inclusions in ruby from Asian marble deposits: Genetic implications. *Eur. J. Mineral.* **2015**, *27*, 393–404. [[CrossRef](#)]
6. Tapponnier, P.; Lacassin, R.; Leloup, P.H.; Schärer, U.; Zhong, D.L.; Wu, H.W.; Liu, X.H.; Ji, S.C.; Zhang, L.S.; Zhong, J.Y. The Ailao Shan/Red River metamorphic belt: Tertiary left-lateral shear between Indochina and South China. *Nature* **1990**, *343*, 431–437. [[CrossRef](#)]
7. Leloup, P.H.; Lacassin, R.; Tapponnier, P.; Schärer, U.; Zhong, D.L.; Liu, X.H.; Zhang, L.S.; Ji, S.C.; Trinh, P.T. The Ailao Shan-Red river shear zone (Yunnan, China), tertiary transform boundary of Indochina. *Tectonophysics* **1995**, *251*, 3–84. [[CrossRef](#)]
8. Leloup, P.H.; Harrison, T.M.; Ryerson, F.J.; Chen, W.J.; Li, Q.; Tapponnier, P.; Lacassin, R. Structural, petrological and thermal evolution of a Tertiary ductile strike-slip shear zone, Diancang Shan, Yunnan. *J. Geophys. Res.* **1993**, *98*, 6715–6743. [[CrossRef](#)]
9. Zhang, L.S.; Schärer, U. Age and origin of magmatism along the Cenozoic Red River shear belt, China. *Contrib. Mineral. Petrol.* **1999**, *134*, 67–85. [[CrossRef](#)]
10. Huang, W.Q.; Ni, P.; Zhou, J.G.; Shui, T.; Pan, J.Y.; Fan, M.S.; Yang, Y.L. Fluid inclusion and titanite U-Pb age constraints on the Yuanjiang ruby mineralization in the Ailao Shan-Red River metamorphic belt, Southwest China. *Can. Mineral.* **2021**. accepted.
11. Leloup, P.H.; Kienast, J.R. High-temperature metamorphism in a major strike-slip shear zone: The Ailao Shan-Red River, People's Republic of China. *Earth Planet. Sci. Lett.* **1993**, *118*, 213–234. [[CrossRef](#)]
12. Cloke, P.L. The geologic role of polysulfides—Part II: The solubility of acanthite and covellite in sodium polysulfide solutions. *Geochim. Cosmochim. Acta* **1963**, *27*, 1299–1319. [[CrossRef](#)]
13. Migdisov, A.A.; Bychkov, A.Y. The behaviour of metals and sulphur during the formation of hydrothermal mercury-antimony-arsenic mineralization, Uzon caldera, Kamchatka, Russia. *J. Volcanol. Geotherm. Res.* **1998**, *84*, 153–171. [[CrossRef](#)]
14. Migdisov, A.A.; Suleimenov, O.M.; Alekhin, Y.V. Experimental study of polysulfane stability in gaseous hydrogen sulfide. *Geochim. Cosmochim. Acta* **1998**, *62*, 2627–2635. [[CrossRef](#)]
15. Garnier, V.; Giuliani, G.; Ohnenstetter, D.; Fallick, A.E.; Dubessy, J.; Banks, D.; Hoàng Quang, V.; Lhomme, T.; Maluski, H.; Pêcher, A.; et al. Marble-hosted ruby deposits from Central and Southeast Asia: Towards a new genetic model. *Ore Geol. Rev.* **2008**, *34*, 169–191. [[CrossRef](#)]
16. Tapponnier, P.; Xu, Z.Q.; Roger, F.; Meyer, B.; Arnaud, N.; Wittlinger, G.; Yang, J.S. Oblique stepwise rise and growth of the Tibet Plateau. *Science* **2001**, *294*, 1671–1677. [[CrossRef](#)] [[PubMed](#)]
17. Yunnan Bureau of Geology and Mineral Resources. *The Census Report of Ruby Deposit from Xiaoyangjie Township, Yuanjiang County, Yunnan Province, 1992*; Yunnan Bureau of Geology and Mineral Resources: Yuxi, China, 1992.
18. Wang, J.H.; Yin, A.; Harrison, T.M.; Grove, M.; Zhang, Y.Q.; Xie, G.H. A tectonic model for Cenozoic igneous activities in the eastern Indo-Asian collision zone. *Earth Planet. Sci. Lett.* **2001**, *188*, 123–133. [[CrossRef](#)]
19. Giuliani, G.; Hoàng Quang, V.; Phan Trong, T.; France-Lanord, C.; Coget, P. Carbon isotopes study on graphite and coexisting calcite-graphite pairs in marbles from the Luc Yen and Yen Bai districts, North of Vietnam. *Bull. Liaison SFMC* **1999**, *11*, 80–82.
20. Huang, W.Q.; Ni, P.; Shui, T.; Pan, J.Y.; Fan, M.S.; Yang, Y.L.; Chi, Z.; Ding, J.Y. Trace element geochemistry and mineral inclusions constraints on the petrogenesis of the marble-hosted ruby deposit from Yuanjiang, China. *Can. Mineral.* **2021**, *59*, 381–408. [[CrossRef](#)]
21. Dzikowski, T.J.; Cempírek, J.; Groat, L.A.; Dipple, G.M.; Giuliani, G. Origin of gem corundum in calcite marble: The Revelstoke occurrence in the Canadian Cordillera of British Columbia. *Lithos* **2014**, *198*, 281–297. [[CrossRef](#)]
22. Wood, S.A.; Pan, P.; Zhang, Y.; Mucci, A. The solubility of Pt and Pd sulfides and Au in bisulfide solutions. *Miner. Depos.* **1994**, *29*, 309–317. [[CrossRef](#)]